J. Phys. G: Nucl. Part. Phys. **34** (2007) 2665–2678 doi:10.1088/0954-3899/34/12/011

High-resolution investigation of the ^{121}Sb(p,t)^{119}Sb reaction and quasiparticle–phonon model description

P Guazzoni[1], L Zetta[1], V Yu Ponomarev[2], G Graw[3], R Hertenberger[3], T Faestermann[4], H-F Wirth[4] and M Jaskóla[5]

[1] Dipartimento di Fisica dell'Università, and Istituto Nazionale di Fisica Nucleare, Via Celoria 16, I-20133 Milano, Italy
[2] Institut für Kernphysik, Technische Universität Darmstadt, Schlossgartenstrasse 9, D-64289 Darmstadt, Germany
[3] Sektion Physik der Universität München, D-85748 Garching, Germany
[4] Physik Department, Technische Universität München, D-85748 Garching, Germany
[5] Soltan Institute for Nuclear Studies, Warsaw, Poland

E-mail: luisa.zetta@mi.infn.it

Received 17 October 2007
Published 16 November 2007
Online at stacks.iop.org/JPhysG/34/2665

Abstract

The ^{121}Sb(p,t)^{119}Sb reaction has been measured in a high-resolution experiment at an incident energy of 21 MeV. Accurate measurement of the (p,t) reaction angular distributions for the transitions to the levels of ^{119}Sb allows us to determine energies of 59 levels, 23 of which have been identified for the first time, and to assign the angular momentum transfer values and a well-defined range for the J values. DWBA analysis has been performed in a finite-range approximation, assuming a dineutron cluster pickup mechanism, by using conventional Woods–Saxon potentials for the entrance proton and exit triton channel. The present (p,t) data have been supplemented by microscopic calculations in the framework of the quasiparticle–phonon model, giving a reasonably good description of the experimental fragmentation of the integrated cross sections and the absence of (p,t) strength above 2.9 MeV.

Communicated by Professor A Covello

1. Introduction

The particle–core weak coupling model is a useful spectroscopic tool for supplementing level structure information obtained by transfer reactions as (p,α) and (p,t).

In our previous work concerning $Z = 40$ [1, 2] and $Z = 50$ [3, 4] regions, it has been observed that in (p,α) and (p,t) reactions on near-magic nuclei having one nucleon outside a completely filled major shell, the unpaired slightly bound nucleon acts as a spectator. The coupling of the odd spectator nucleon with an excited state of the core generates a multiplet

of states with spin J, whose excitation probability is proportional to $2J + 1$. The spin J varies from $|J_p - J_C|$ to $J_p + J_C$, where $J_p(J_C)$ is the spin of the nucleon (core).

To further investigate the systematics of this coupling we have measured the (p,t) reaction on ^{121}Sb target, an odd proton nucleus with a ground-state spin of 5/2, where the $1d_{5/2}$ proton configuration is expected to be dominant (77%) as shown by the calculations performed by Hooper *et al* [5]. The core reaction ^{120}Sn(p,t)^{118}Sn was also studied in the same experimental conditions to obtain information, via cross-section comparison, on the role of the extra unpaired proton [6].

The level structure of ^{119}Sb nucleus has been evidenced by different kinds of experimental measurements. To fully and unambiguously characterize both low- and high-spin states, it is very important to dispose of a large amount of experimental data. In fact the combined use of various techniques, such as γ-ray spectroscopy, with both selective and non-selective reactions, β decay, radiative decay and transfer reactions allows us to fulfil this aim.

In studies of radioactive decays of ^{119m}Sb [7, 8] and ^{119g}Sb [9], the half lives of some low-lying states of ^{119}Sb have been determined by means of a delayed coincidence method and $\gamma\gamma$ angular correlation measurements, and the level scheme of ^{119}Sb has been proposed [9].

The states excited in ^{119}Sb nucleus have been investigated from ^{119}Sn(p,n)^{119}Sb reaction by Kernell *et al* [10] via the direct measurement of neutrons from the 0^+ analogue state. In the (p,nγ) reaction [11], de-excited states of ^{119}Sb have been studied from γ-ray spectroscopy and a number of residual states in ^{119}Sb, populated predominantly by the emission of neutrons from the 0^+ analogue state, have been identified.

In ^{119}Sb the fragmentation and splitting of Gamow–Teller strength has been investigated and discussed in a framework of a systematic study of the (^{3}He,t) charge-exchange reaction on essentially all stable Sn isotopes [12].

Population of intrinsic high-spin states as well as the low-lying states has been studied with the ^{116}Sn(α,p)^{119}Sb reaction [13].

The properties of high-spin states in ^{119}Sb, as well as in $^{113-117}$Sb, have been studied via the ^{A}Cd(^{6}Li,3nγ)$^{A+3}$Sb reaction [14]. In beam measurements of γ-ray excitation functions, $\gamma\gamma$ coincidences, γ-ray angular distributions and pulsed-beam-γ timing spectra were carried out to obtain level energies, decay schemes, γ-ray multipolarities, J^π assignments and isomeric lifetimes. High-spin states in ^{119}Sb nucleus and collective structures have been investigated via γ-ray studies with the heavy ion fusion–evaporation ^{116}Cd(^{7}Li,4nγ)^{119}Sb reaction [15]. The level scheme of ^{119}Sb was constructed from the coincidence data. A combination of γ-ray coincidence relationships, intensity balances and energy sums allowed the placement of transitions.

The fusion–evaporation reactions induced by heavy ions very selectively populate the high-spin states; orbital angular momentum transfer as large as $17\hbar$ can be, for example, achieved with 34 MeV ^{6}Li, and the dominant γ-ray decay mode of the residual nucleus is through yrast states.

Transfer reactions, on the contrary, characterize low-spin states: one-nucleon transfer reactions almost exclusively feed the single-particle component of the final states, and two-nucleon transfer reactions evidence at low-excitation energy the correlations associated with the pairing interaction. As a consequence, the two kinds of reactions, (HI,xnγ) and transfer reactions, are complementary not only in their capability of selecting particular states, but also in their spin and parity ranges.

The only transfer reaction reported in literature [16] is the ^{118}Sn(^{3}He,d)^{119}Sb reaction, measured at 19 MeV by Kantele *et al* [17], at 28.2 MeV by Ishimatsu *et al* [18] and at 18 MeV

by Conjeaud *et al* [19]. In [18, 19], the angular momentum transfers for eight transitions are given.

The ^{121}Sb(p,t)^{119}Sb reaction was never measured before the present work, apart from the very preliminary results obtained at 26 MeV by our group at 10° and reported by Evaluated Nuclear Data Structure Data File (ENSDF, supported by the National Nuclear Data Center, Brookhaven National Laboratory) [20].

The present study of the ^{121}Sb(p,t)^{119}Sb reaction is aimed to characterize the low-spin states of ^{119}Sb by means of a high-resolution experiment.

In connection with the experimental work, we have performed theoretical investigations on ^{119}Sb employing the quasiparticle–phonon model (QPM) approach for nuclear structure calculations.

QPM [21] accounts for the interaction between simple (one-quasiparticle) and complex (quasiparticle $\times$ n-phonons) configurations of nuclear excitations, and rather successfully describes the fragmentation of the simplest components of nuclear wavefunctions [21–24]. Within QPM by solving quasiparticle random-phase approximation equations, phonons of different multipolarities and parities are obtained. The single-particle spectrum and phonon basis are obtained from the calculations on the neighboring even–even nuclear core. The QPM analysis can be transformed into the spectator approach by switching off the interaction between different configurations in the model space.

In section 2, the experimental procedure is described. In section 3, the measured cross-section angular distributions are compared with the distorted wave Born approximation (DWBA) analysis with conventional Woods–Saxon potentials. Section 4 deals with the QPM analysis of the experimental integrated cross sections. Finally, section 5 presents a summary of our conclusions.

2. Experimental procedure

The ^{121}Sb(p,t)^{119}Sb reaction has been measured using the 21 MeV proton beam delivered by the HVEC MP Tandem accelerator of the Maier–Leibnitz Laboratory of Ludwig Maximilians University and Technical University of Munich. The ^{121}Sb isotopic enriched (99.53%) target had a thickness of 102 μg cm^{-2} deposited on a 10 μg cm^{-2} carbon backing. The bright Stern–Gerlach polarized ion source was used with unpolarized hydrogen [25]. The beam current intensity was up to 500 nA.

The reaction products were analyzed with the Munich Q3D spectrograph [26] at 11 angles from 10° up to 65° in different magnetic field settings such as to reach an excitation energy of the ^{119}Sb residual nucleus of 2.874 MeV, the magnetic field values being chosen in such a way to have overlaps in energy.

In figure 1, the measured triton spectrum at 20° is shown and the excitation energies of the most part of levels are indicated.

The acceptance opening of the magnetic spectrograph was 11.04 msr (horizontal $\times$ vertical of $\pm$20 mm $\times$ $\pm$20 mm) for $\theta \geqslant 10°$.

The analyzed particles were detected in the 1.8 m long focal plane detector [27] which consists of an array of single-wire proportional counters with an additional cathode readout structure, followed by a plastic scintillator for particle identification. This device provides focal plane reconstruction, good position resolution and good background suppression using ΔE–E particle identification via the energy-loss signals on wires and the signals produced by the particles stopped in the plastic scintillator. The excellent energetic characteristics of the accelerator, the Q3D and the detector enable us to measure high-precision and high-resolution excitation spectra, with an energy resolution of about 8 keV full width at half maximum in the

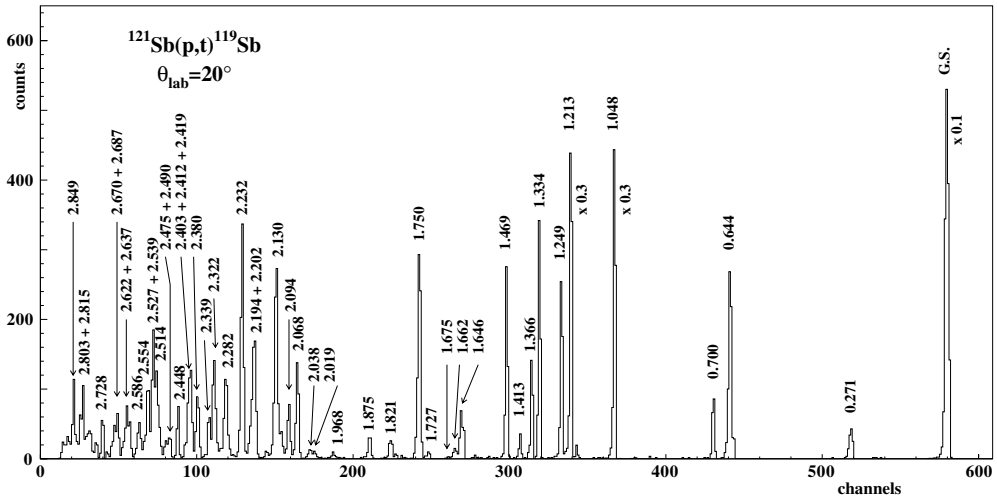

Figure 1. Position spectrum of tritons measured at $\theta = 20°$. The excitation energies in MeV of some levels are indicated.

detection of the outgoing tritons. The energy calibration of the spectra of the ^{121}Sb(p,t)^{119}Sb reaction has been carried out using polynomials of rank three. The polynomial parameters were set by reproducing well-known excitation energies of ^{119}Sb levels determined in γ-decay experiments [28]. Our quoted energies are estimated at 3 keV.

Absolute cross sections have been calculated taking into account the effective target thickness, solid angle, collected charge and were estimated with an uncertainty of $\sim$15%.

The triton spectra were analyzed by means of the computer code AUTOFIT [29] using as reference the shape of the triton peak at 2.232 MeV.

The high resolving power of the Q3D, the very low background, the large solid angle, the favorable peak to background ratio and the spectrum energy resolution allowed measurement of rather weakly populated levels having cross-section values as low as 1 μb sr^{-1} at the maximum of the angular distribution.

We have measured 59 transitions to the final states of ^{119}Sb up to $E_x = 2.874$ MeV, of which 23 have been observed for the first time. Most of the states identified in the present experiment are weakly excited. The large number of weak transitions confirms the selectivity of (p,t) reactions which populate a small number of intense transitions.

The angular momentum transferred, the spin value range and the parity have been assigned for all the observed levels by means of the DWBA analysis reported in section 3.

Table 1 summarizes the results obtained in the present experiment: the energy, spin and parity of the ^{119}Sb levels adopted so far [28] are listed together with the energy, the angular momentum transfer, the spin range and the parity observed in the present study of ^{121}Sb(p,t)^{119}Sb reaction. The integrated experimental cross sections, estimated with a systematic error of 15%, are also reported in the last column of table 1, together with the statistical errors.

3. Experimental results

In general, more than one L-transfer contributes to a given final state in the (p,t) reaction from nonzero-spin target, as in the present case of ^{121}Sb(p,t)^{119}Sb reaction. As a consequence, the

Table 1. The adopted energies, spins and parities of the ^{119}Sb levels in comparison with the results of the present work: the energies, the transferred angular momentum L, the spin and parity range and the integrated cross sections from 7.5° to 67.5°. Our quoted energies are estimated to have an uncertainty of ±3 keV. Absolute cross sections are estimated with a systematic uncertainty of ±15% and reported with the statistical error.

Adopted		Present experiment			
E_{exc} (keV)	J^π	E_{exc} (MeV)	L_{tran}	J^π	σ_{int} (μb)
0.0	$5/2^+$	0.0	0	$5/2^+$	2371 ± 17
270.52	$7/2^+$	0.271	4	$(3/2-13/2)^+$	5.0 ± 0.9
644.03	$1/2^+$	0.644	2	$(1/2-9/2)^+$	26 ± 2
699.88	$3/2^+$,$5/2^+$	0.700	2	$(1/2-9/2)^+$	8.8 ± 1.2
970.90	$9/2^+$				
1048.42	$7/2^+$	1.048	2	$(1/2-9/2)^+$	149 ± 5
1212.74	$9/2^+$	1.213	2	$(1/2-9/2)^+$	159 ± 5
1249.74	$9/2^+$	1.250	2	$(1/2-9/2)^+$	29 ± 2
1327.25	$(1/2^-)$				
1338.61	$3/2^+$	1.334	2	$(1/2-9/2)^+$	44 ± 3
1340.75	$11/2^+$				
1366.34	$11/2^-$	1.366	5	$(5/2-15/2)^-$	29 ± 2
1407.35	$11/2^+$				
1413.21	$3/2^-$	1.413	3	$(1/2-11/2)^-$	3.8 ± 0.8
1450					
1469	$3/2^+$,$5/2^+$	1.469	2	$(1/2-9/2)^+$	28 ± 2
1482	$1/2^-$				
1487.61	$(3/2^+)$				
1547					
1646.5	$1/2^+$				
		1.646	0	$5/2^+$	25 ± 1
1660	$(7/2^+)$				
		1.662	2	$(1/2-9/2)^+$	3.5 ± 0.5
1665	$(3/2^+,5/2^+)$				
1675.72	$13/2^+$	1.675	4	$(3/2-13/2)^+$	0.8 ± 0.2
1730		1.727	2	$(1/2-9/2)^+$	1.7 ± 0.4
1749.64	$3/2^+$	1.750	2	$(1/2-9/2)^+$	41 ± 2
1821.14	$1/2^+$	1.821	2	$(1/2-9/2)^+$	3.0 ± 0.4
1848.2					
1875.32	$(1/2^+,3/2)$	1.875	2	$(1/2-9/2)^+$	5.3 ± 0.6
1970	$7/2^+$,$9/2^+$	1.968	4	$(3/2-13/2)^+$	2.0 ± 0.4
1982.0					
		2.019	4	$(3/2-13/2)^+$	2.8 ± 0.4
2037.61	$15/2^+$				
2043		2.038	5	$(5/2-15/2)^-$	3.4 ± 0.5
2067		2.068	4	$(3/2-13/2)^+$	27 ± 1
2094.38		2.094	2 + 4 + 6	$(7/2,9/2)^+$	14 ± 1
2100					
2114	$1/2^+$,$3/2^+$,$5/2^+$	2.114	4	$(3/2-13/2)^+$	12 ± 1
2129.82	$9/2^-$	2.130	3	$(1/2-11/2)^-$	53 ± 2
2130					
2138.38	$13/2^+$	2.138	6	$(7/2-17/2)^+$	3.0 ± 0.5
2159		2.162	3	$(1/2-11/2)^-$	2.1 ± 0.4
2187		2.194	2 + 4 + 6	$(7/2,9/2)^+$	40 ± 2

Table 1. (Continued.)

Adopted		Present experiment			
E_{exc} (keV)	J^{π}	E_{exc} (MeV)	L_{tran}	J^{π}	σ_{int} (μb)
2202.35	$13/2^+$	2.202	6	$(7/2-17/2)^+$	11 ± 1
2223					
2226.06	$11/2^-$	2.232	3	$(1/2-11/2)^-$	64 ± 2
2258					
2269.1	$1/2^+,3/2^+,5/2^+$				
2278.93	$13/2^-$				
2283.7	$9/2^-$	2.282	3	$(1/2-11/2)^-$	19 ± 2
2298		2.294	2	$(1/2-9/2)^+$	3.1 ± 0.4
2314.02	$(15/2)^-$				
2320		2.322	2 + 4 + 6	$(7/2,9/2)^+$	33 ± 2
2327					
		2.339	3	$(1/2-11/2)^-$	11 ± 1
2355					
2360.20	$9/2^-$				
2379.60	(9/2,13/2)				
2384		2.380	2 + 4 + 6	$(7/2,9/2)^+$	22 ± 1
		2.403	3	$(1/2-11/2)^-$	23 ± 1
		2.412	3 + 5 + 7	$(9/2,11/2)^-$	11 ± 1
2415.53	$1/2^+$				
2419.34	$17/2^+$	2.419	6	$(7/2-17/2)^+$	2.4 ± 0.4
		2.448	0	$5/2^+$	13 ± 1
2455					
2475.44	$15/2^-$				
		2.475	3 + 5 + 7	$(9/2,11/2)^-$	8.2 ± 0.7
		2.490	4	$(3/2-13/2)^+$	5.2 ± 0.6
2505.24	$15/2^-$				
2508		2.514	1	$(3/2-7/2)^-$	17 ± 1
		2.527	0	$5/2^+$	33 ± 2
2539		2.539	2	$(1/2-9/2)^+$	23 ± 1
2553.6	$(19/2^-)$				
2561		2.554	3	$(1/2-11/2)^-$	20 ± 1
		2.586	3 + 5 + 7	$(9/2,11/2)^-$	13 ± 1
2624		2.622	3 + 5 + 7	$(9/2,11/2)^-$	14 ± 1
		2.637	2	$(1/2-9/2)^+$	11 ± 1
		2.670	3 + 5 + 7	$(9/2,11/2)^-$	15 ± 1
		2.687	3 + 5 + 7	$(9/2,11/2)^-$	7.3 ± 0.7
2707.74	$17/2^-$				
2708	$1/2^+,3/2^+,5/2^+$				
		2.728	2	$(1/2-9/2)^+$	11 ± 1
2747.68					
2749					
		2.755	4	$(3/2-13/2)^+$	6.1 ± 0.6
2769.08	$(17/2^+)$				
		2.777	3	$(1/2-11/2)^-$	7.6 ± 0.7
		2.788	3	$(1/2-11/2)^-$	8.2 ± 0.7
		2.803	3 + 5 + 7	$(9/2,11/2)^-$	23 ± 1
		2.815	9	$(13/2-23/2)^-$	12 ± 1
		2.829	3	$(1/2-11/2)^-$	5.2 ± 0.6

Table 1. (Continued.)

Adopted		Present experiment			
E_{exc} (keV)	J^{π}	E_{exc} (MeV)	L_{tran}	J^{π}	σ_{int} (μb)
2841.7	$(21/2^{-})$				
2841.7	$(27/2^{+})$				
2848.99	$19/2^{+}$				
		2.849	5	$(5/2-15/2)^{-}$	23 ± 1
2862					
		2.874	2	$(1/2-9/2)^{+}$	7.5 ± 0.7
2885					

Table 2. Woods–Saxon optical model parameters for the incident proton, the outgoing triton and the geometrical parameters for the bound–state of the transferred dineutron cluster. As usual, the potential values are in MeV, and the radius and diffuseness values in fm.

	V_r	r_r	a_r	W_v	r_v	a_v	W_d	r_d	a_d	V_{so}	r_{so}	a_{so}	r_c
p	50.0	1.25	0.65				10.0	1.30	0.60	3.00	1.25	0.70	1.25
t	176.0	1.14	0.72	18.0	1.61	0.82				8.00	1.10	0.80	1.30
B.S.		1.30	0.50										

angular distribution will be composed of all the allowed L-transfers, whose contributions must be incoherently added.

When only one L-transfer dominates a given transition amplitude, the situation is more favorable and the accuracy of the spectroscopic information is higher. The (p,t) reactions on odd A-nuclei display such behavior for a class of states arising from the coupling of the odd particle with the states of the (A-1) even–even core [4, 30, 31].

The measured differential cross sections display two kinds of shapes: one exhibits relevant angular structure, significant enough to allow different L-transfers to be distinguished; the other, rather featureless, is distinctive of more L-transfer contributions.

The DWBA analysis of the experimental angular distributions has been carried out assuming a semimicroscopic dineutron cluster pickup. The calculations have been performed using the computer code TWOFNR [32] in a finite-range approximation. A proton–dineutron interaction potential of gaussian form $V(r_{p2n}) = V_0 \exp[-(r_{p2n}/\xi)^2]$ with $\xi = 2$ fm has been used. The parameters for the proton entrance channel have been deduced from a systematic survey of elastic scattering by Perey [33] and for the triton exit channel by Fleming [34]. Table 2 summarizes the optical model parameters for the proton and triton elastic scattering, used in the Woods–Saxon parameterization, and the geometric parameters for evaluating the bound-state wavefunction of the transferred dineutron cluster.

These optical model parameters have been also used to analyze the angular distributions of the ^{122}Sn(p,t)^{120}Sn reaction measured at 20 MeV [34] and 26 MeV [35, 36], the ^{120}Sn(p,t)^{118}Sn [6] measured at 21 MeV, the ^{116}Sn(p,t)^{114}Sn measured at 26 MeV [37], the ^{112}Sn(p,t)^{110}Sn measured at 26 MeV [38] and ^{123}Sb(p,t)^{121}Sb reaction measured at 26 MeV [4], giving good agreement between experimental results and DWBA calculations. Good agreement between experimental results and DWBA calculations has been also achieved for the present ^{121}Sb(p,t)^{119}Sb reaction allowing the assumption that multistep process is small for this reaction. Thus, multistep processes are not taken into account in the present DWBA analyses.

Transferred angular momentum L has been assigned by comparing the shapes of the experimental $d\sigma/d\Omega$ with the calculated ones. The experimental- and DWBA-calculated

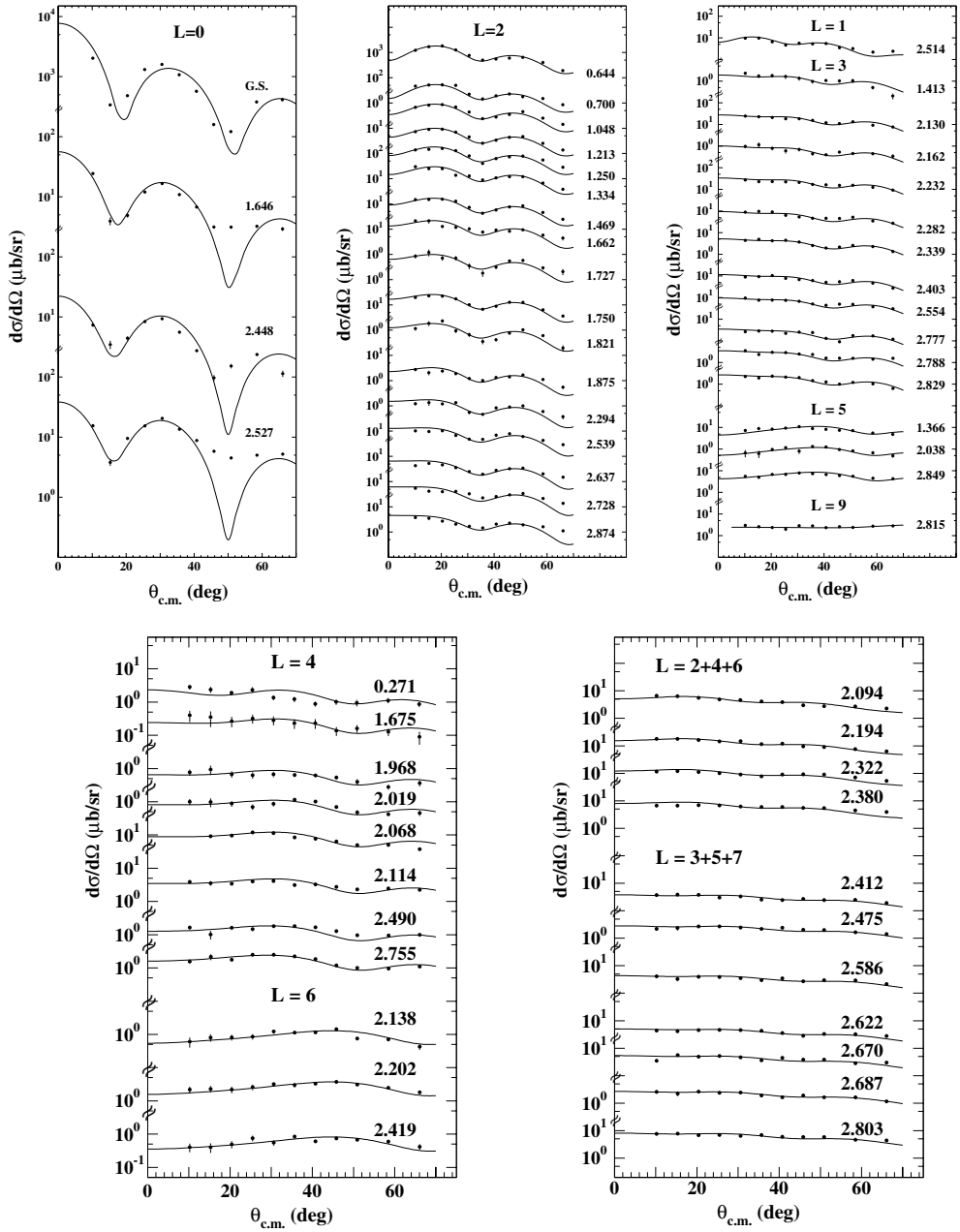

Figure 2. Experimental and calculated angular distributions for all the identified levels. The excitation energies (MeV) and L-transfer values are indicated.

angular distributions for all the observed levels are reported in figure 2. As table 1 evidences, we have determined the angular momentum transfers and assigned the parity for all the observed levels.

Generally we are able to fit rather satisfactorily the angular distributions of many of the observed transitions assuming only one L-transfer. Eleven transitions show a rather featureless

angular distribution which cannot be reproduced with a unique L-transfer, but is distinctive of more L-transfer contributions: 2.094, 2.194, 2.322, 2.380, 2.412, 2.475, 2.586, 2.622, 2.670, 2.687 and 2.803 MeV.

We have no *a priori* argument to choose the L-transfer mixing, but we may classify the shapes of the angular distributions of these 11 levels in two classes: 2.094, 2.194, 2.322 and 2.380 MeV levels belong to the first class, whereas 2.412, 2.475, 2.586, 2.622, 2.670, 2.687 and 2.803 MeV levels to the second one.

The experimental angular distributions of the first class levels are well reproduced by a combination of $L = 2+4+6$. The results of DWBA calculations for these L-values have been incoherently added with a weighting factor proportional to $2L + 1$, following the analysis of Ball [39], and as already done in the analysis of ^{123}Sb(p,t)^{121}Sb reaction [4] and ^{91}Zr(p,t)^{89}Zr [40]. Although individual L-transfer distributions display noticeable angular structure, the shape of the composite angular distribution possesses little angular structure.

A similar treatment of the angular distributions of the second class levels, for which the mixing of $L = 3+5+7$ is considered, produces featureless angular distributions agreeing well with the experimental ones.

The levels of the first class 2.094, 2.194, 2.322 and 2.380 MeV with $J^\pi = 7/2^+, 9/2^+$ probably may correspond to the following levels reported on Nuclear Data Sheets compilation (NDS) [28] without spin and parity assignment, at 2094.38, (2187 ± 10), 2320 and 2384 keV, respectively.

Among the levels of the second class, with $J^\pi = 9/2^-, 11/2^-$, the 2.412 and 2.475 MeV probably cannot coincide with the levels reported by NDS [28] at 2415.53 keV with $J^\pi = 1/2^+$ and at 2475.44 keV with $J^\pi = 15/2^-$. The remaining levels at 2.586, 2.622, 2.670, 2.687 and 2.803 MeV are observed for the first time in the present experiment.

For the levels up to 1.469 MeV we confirm the parity assignments reported on NDS [28], whereas the adopted spin values are in the range allowed by the L-transfer values assigned by the present study and reported in table 1. In the excitation energy region up to 2.527 MeV the following levels, besides the ground state, are observed to exhibit an angular distribution characteristic of $L = 0$ transfer: 1.646, 2.448 and 2.527 MeV. Since the ground state of ^{121}Sb is $5/2^+$, these $L = 0$ transitions uniquely identify the previous states as $5/2^+$ levels. The 1.646 MeV $5/2^+$ level observed in the present experiment presumably does not correspond to the level reported in NDS [28] at 1646.5 keV with $J^\pi = 1/2^+$. The two levels at 2.448 and 2.527 MeV are observed for the first time in this measurement.

An $L = 5$ transfer, $5/2^- < J^\pi < 15/2^-$, well reproduces the angular distribution corresponding to the transition to the level at 2.038 MeV which presumably does not coincide with the level at 2037.61 keV with $J^\pi = 15/2^+$. The level we observe corresponds to the level at 2.043 MeV reported on NDS, from our very preliminary results concerning the ^{121}Sb(p,t)^{119}Sb reaction [20], without spin and parity assignment.

The level we observe at 2.849 MeV whose angular distribution is well reproduced by $L = 5$ transfer probably does not correspond to the level reported on NDS [28] at 2848.99 keV with $J^\pi = 19/2^+$.

4. Theoretical analysis

Since the analysis of the experimentally measured angular distributions does not allow us to identify the spin of the most of the excited levels in ^{119}Sb, microscopic calculations of the ^{121}Sb(p,t)^{119}Sb reaction integrated cross sections have been performed. The quasiparticle–phonon model (QPM) [21] has been used for this purpose. Ground and excited states in

odd-mass nuclei are described in this model by a wavefunction which contains quasiparticle-, and different (quasiparticle $\times$ n-phonon) configurations.

The most complex configurations employed in the present calculations are (quasiparticle $\times$ 2-phonon) ones. Thus, the wavefunction of the states in ^{119}Sb has the form

$$\Psi^{\nu}(JM) = \left\{ C^{\nu}(J)\alpha^{+}_{JM} + \sum_{jLi} S^{\nu}_{jLi}(J)\left[\alpha^{+}_{j} Q^{+}_{Li}\right]_{JM} + \sum_{jL_1i_1L_2i_2l} D^{\nu}_{jL_1i_1L_2i_2}(J) \frac{\left[\alpha^{+}_{j}\left[Q^{+}_{L_1i_1} Q^{+}_{L_2i_2}\right]_{l}\right]_{JM}}{\sqrt{1+\delta_{L_1i_1,L_2i_2}}} \right\} |^{118}\mathrm{Sn}\rangle_{g.s.}, \tag{1}$$

where α^{+}_{jm} is a quasiparticle creation operator, $Q^{+}_{L\mu i}$ is a phonon excitation of the ^{118}Sn core, [...] means a vector coupling of operators and $|^{118}\mathrm{Sn}\rangle_{g.s.}$ is the wavefunction of the ^{118}Sn ground state which is considered as a phonon vacuum.

An unpaired quasiparticle in (1) has fermion quantum numbers $jm = |nljm\rangle$ the proton mean field which is described by the Woods–Saxon potential with parameters from [41]. The phonons $Q^{+}_{L\mu i}$ are quasi-bosons with integer value of the angular momentum L. They are built up from different proton and neutron two-quasiparticle configurations. Their internal fermion structure and excitation energies are obtained from solving quasiparticle-RPA equations ($i = 1, 2, \ldots$, means the lowest in energy, next to the lowest, etc RPA-solution).

The coefficients C, S and D in (1) and eigen energies of the states in odd-mass nuclei are obtained by diagonalization of the model Hamiltonian on the set of wavefunctions (1). Diagonalization is performed for each value of the total angular momentum J and index ν in equation (1) means the order number of a state for each J.

Assuming one-step mechanism of the (p,t) reaction, the ^{121}Sb(p,t)^{119}Sb cross section to the final state $J\nu$ by the momentum transfer L has the form

$$\frac{\mathrm{d}\sigma}{\mathrm{d}\Omega}(^{121}\mathrm{Sb}_{g.s.} \rightarrow {}^{119}\mathrm{Sb}_{J\nu}) = \left| C^{\nu}(J)\delta_{J,5/2^+}A_{g.s.} + \sum_{i} S^{\nu}_{jLi}(J)\delta_{j,5/2^+}A_{Li} \right|^2, \tag{2}$$

where $J = 5/2^+$, $\nu = 1$ is the ground state of ^{119}Sb. When the ^{119}Sb is excited the same set of phonons of the core ^{118}Sn is involved, and the unpaired proton of antimony does not influence the excitation process in a one-step transfer. Since experimental data for the ^{120}Sn(p,t)^{118}Sn reaction in a very similar conditions to the ^{121}Sb(p,t)^{119}Sb reaction are available, one may use the data from the first reaction in expression (2). Then, $A_{g.s.}$ in (2) corresponds to the transition between the ground states $^{120}\mathrm{Sn}_{g.s.} \rightarrow {}^{118}\mathrm{Sn}_{g.s.}$ and A_{Li} equals the amplitude of excitation of one-phonon configuration Q^{+}_{Li} in ^{118}Sn.

To extract A_{Li} from the data, the calculation in even–even ^{118}Sn have been performed. We have used a wavefunction of excited states in this nucleus of the same complexity as in odd ^{119}Sb, i.e. it contains one- and two-phonon components:

$$\Psi^{\nu}(LM) = \left\{ \sum_{i} R^{\nu}_{Ji} Q^{+}_{JMi} + \sum_{L_1i_1L_2i_2} T^{\nu}_{L_1i_1L_2i_2}(J) \frac{\left[Q^{+}_{L_1i_1} Q^{+}_{L_2i_2}\right]_{LM}}{\sqrt{1+\delta_{L_1i_1,L_2i_2}}} \right\} |^{118}\mathrm{Sn}\rangle_{g.s.} \tag{3}$$

The cross section of the $^{120}\mathrm{Sn}_{g.s.}$(p, t)$^{118}\mathrm{Sn}_{LMi}$ reaction has the form

$$\frac{\mathrm{d}\sigma}{\mathrm{d}\Omega}(^{120}\mathrm{Sn}_{g.s.} \rightarrow {}^{118}\mathrm{Sb}_{J\nu}) = \left| \sum_{i} R^{\nu}_{Li} A_{Li} \right|^2. \tag{4}$$

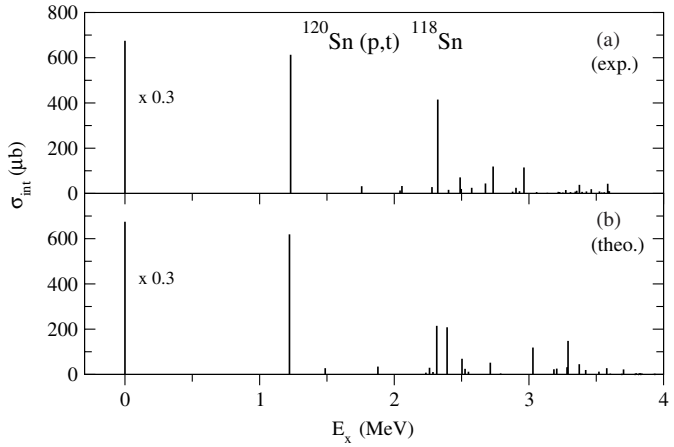

Figure 3. Comparison between the experimental integrated cross sections of the ^{120}Sn(p,t)^{118}Sn reaction (a) and the calculated ones (b). The calculations are performed with the wavefunction (3).

Coefficients R in equations (3) and (4) have been obtained from diagonalization of the model Hamiltonian on the set of wavefunctions (3) and amplitudes A_{Ji} have been varied to reach the best agreement between calculation and experiment for each multipolarity L.

Comparing the wavefunctions used in the calculations of even and odd nuclei, one may note that keeping in the second and third terms of equation (1) only configurations in which unpaired quasiparticle is located on the same level as in the first term (i.e. inserting $\delta_{j,J}$ in the second and third terms) and switching off the term in the model Hamiltonian responsible for quasiparticle–phonon scattering, we obtain a simplified approach in which the quasiparticle is considered as a pure spectator.

In figure 3, the experimental integrated cross sections of the ^{120}Sn(p,t)^{118}Sn reaction (a) are compared with the calculations (b) performed with the wavefunction (3).

In figure 4, the experimental integrated cross sections of the ^{121}Sb(p,t)^{119}Sb reaction (a) are compared with the complete calculations (c) performed with the wavefunction (1) and within the simplified (spectator) approach (b). In the spectator approach, all multiplets $\left[\alpha^+_J Q^+_{Li}\right]_J$ with $|J - L| \leqslant J \leqslant (J + L)$ are energy degenerate and only the states with a maximum possible value of J are seen because of their larger cross sections.

The spectator approach reproduces the general features of the experimental distribution, but strongly underestimate the observed reaction cross-section fragmentation over the energy interval. The description of data is substantially improved in the realistic calculations with the wavefunction (1). The theory reasonably well reproduces the fragmentation of the (p,t) cross section at higher excitation energy and the absence of the (p,t) strength above 2.9 MeV. Below 2 MeV, the states are excited mostly via $\left[\alpha^+_j \times 2^+_1\right]_J$ components of their wavefunctions. At higher excitation energies (i.e. between 2 and 3 MeV), many components of the wavefunction play an essential role in the excitation process including configurations with phonons of high multipolarity $\left[\alpha^+_j \times 4^+\right]_J$ and $\left[\alpha^+_j \times 5^-\right]_J$.

In the excitation energy region up to 2.597 MeV, besides the ground state, three $5/2^+$ states have been identified because of $L = 0$ transfer. The corresponding experimental integrated cross sections are plotted in figure 5(a). The theory also predicts the existence of only four $5/2^+$ states below 2.9 MeV, cross sections of their excitation are shown in figure 5(b). The

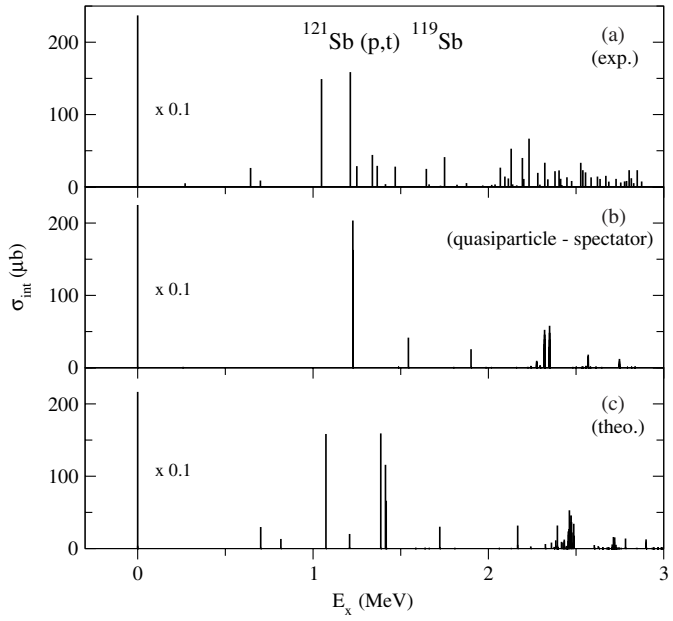

Figure 4. Experimental integrated cross sections of the ^{121}Sb(p,t)^{119}Sb reaction (a) are compared with the complete reaction calculations (c) performed with the wavefunction (1) and with the simplified (spectator) approach (b).

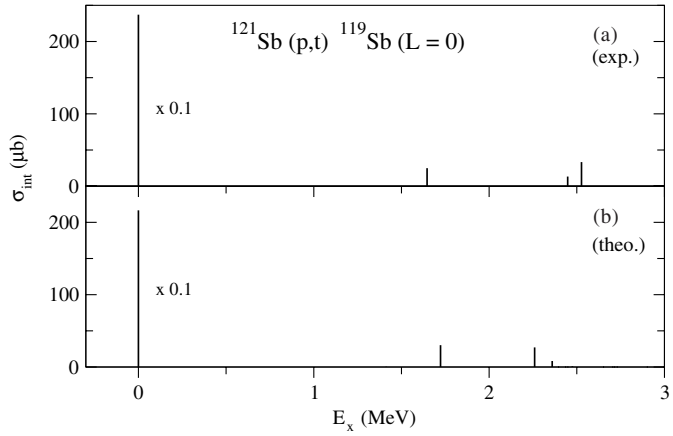

Figure 5. Experimental (a) and QPM (b) integrated cross sections of the four $5/2^+$ ($L = 0$) states below 2.9 MeV of ^{119}Sb excitation energy.

agreement between experiment and theory for these states, in position and integrated (p,t) cross sections, is very good.

5. Summary

The ^{121}Sb(p,t)^{119}Sb reaction has been studied in a high-resolution experiment carried out at an incident proton energy of 21 MeV. Cross section angular distributions have been measured

for 59 transitions to levels of ^{119}Sb up to an excitation energy of 2.874 MeV of which 23 have been observed for the first time.

The transferred angular momentum, the parity and the total spin J range values for all the observed levels have been assigned by a DWBA analysis, assuming a semi-microscopic dineutron cluster pickup mechanism. The calculations have been performed in finite-range approximation, using conventional Woods–Saxon potentials for proton entrance and triton exit channels. Generally, we are able to reproduce rather satisfactorily the angular distributions of many of the observed transitions assuming only one L-transfer. Eleven transitions show a rather featureless angular distribution which cannot be reproduced with a unique L-transfer, but is characteristic of more L-transfer contributions.

For a better understanding of the ^{119}Sb nucleus, we have carried out a theoretical study of ^{119}Sb within the framework of QPM. The present (p,t) experimental data have been supplemented by microscopic calculations, giving a reasonably good reproduction of the experimental fragmentation of cross sections and the absence of (p,t) strength above an excitation energy of 2.9 MeV.

Four experimental $5/2^+$ states identified in the energy range between 0 and 2.6 MeV are well reproduced by the theoretical calculations not only in regard to their energies, but also in regard to the number and the integrated cross sections.

Simplified calculations, in which the unpaired quasiparticle is considered as a pure spectator, reproduce the general features of the experimentally observed distribution of the (p,t) cross section to low-lying levels in ^{119}Sb. In contrast, the spectator approach fails to describe the fragmentation of the cross sections.

Acknowledgments

V Yu P acknowledges support by the DFG under the contract SFB 634.

References

[1] Guazzoni P *et al* 1997 *Z. Phys.* A **356** 381
[2] Guazzoni P *et al* 1998 *Eur. Phys.* A **1** 365
[3] Guazzoni P, Zetta L, Bayman B F, Covello A, Gargano A, Graw G, Hertenberger R, Wirth H-F and Jaskóla M 2005 *Phys. Rev.* C **72** 044604
[4] Guazzoni P, Jaskóla M, Ponomarev V Yu, Zetta L, Graw G, Hertenberger R and Staudt G 2000 *Phys. Rev.* C **62** 054312
[5] Hooper H R, Green P G, Siefken H E, Neilson G C, McDonald W J, Sheppard D M and Dawson W K 1979 *Phys. Rev.* C **20** 2941
[6] Guazzoni P, Zetta L, Graw G, Hertenberger R, Wirth H-F and Jaskóla M 2006 *Maier–Leibnitz Laboratorium Annual Report Universität München* pp 10
[7] Duffait R, Charvet A and Chery R 1975 *Z. Phys.* A **273** 315
[8] Yambe M, Fujioka M, Katakura J, Hayashibe S and Ishimatsu T 1977 *Nucl. Phys.* A **281** 149
[9] Duffait R, Charvet A and Chery R 1975 *Z. Phys.* A **273** 321
[10] Kernell R L, Kim H J, Robinson M L and Johnson C H 1971 *Nucl. Phys.* A **176** 449
[11] Pal J, Dey C C, Bose S, Sinha B K, Chatterjee M B and Mahapatra D P 1994 *Phys. Rev.* C **50** 99
[12] Pham K *et al* 1995 *Phys. Rev.* C **51** 526
[13] Smith P A, Emigh R A, DiGiacomo N J, Smith G R and Peterson R J 1979 *Phys. Rev.* C **19** 1767
[14] Shroy R E, Gaigalas A K, Schatz G and Fossan D B 1979 *Phys. Rev.* C **19** 1324
[15] LaFosse D R, Fossan D B, Hughes J R, Liang Y, Schnare H, Vaska P, Waring M P and Zhang J-y 1997 *Phys. Rev.* C **56** 760
[16] Ohya S and Kitao K 2000 *Nucl. Data Sheets* **89** 345
[17] Kantele J, Hattula J, Hattula T, Kalm H and Marttila O J 1967 *Ann. Acad. Sci. Fenn. Ser.* A **6** 259
[18] Ishimatsu T, Yagi K, Ohmura H, Nakajima Y, Nakagawa T and Orihara H 1967 *Nucl. Phys.* A **104** 481

[19] Conjeaud M, Harar S and Cassagnou Y 1969 *Nucl. Phys.* A **129** 10
[20] ENSDF data base ^{121}Sb(p,t)^{119}Sb 1999 http://www.nndc.bnl.gov
[21] Soloviev V G 1976 *Theory of Complex Nuclei* (Oxford: Pergamon)
[22] Soloviev V G, Stoyanov Ch and Vdovin A I 1980 *Nucl. Phys.* A **342** 261
[23] Vdovin A I, Soloviev V G and Stoyanov Ch 1974 *Yad. Fiz.* **20** 1131
[24] Thao N D, Soloviev V G, Stoyanov Ch and Vdovin A I 1984 *J. Phys. G: Nucl. Phys.* **10** 517
[25] Hertenberger R, Metz A, Eisermann Y, El Abiary K, Ludewig A, Pertl C, Trieb S, Wirth H-F, Schiemenz P and Graw G 2005 *Nucl. Instrum. Methods Phys. Res.* A **536** 266
[26] Loeffler M, Scheere H J and Vonach H 1973 *Nucl. Instrum. Methods* **111** 1
[27] Zanotti E, Bisenberger M, Hertenberger R, Kader H and Graw G 1991 *Nucl. Instrum. Methods Phys. Res.* A **310** 706
[28] Ohya S and Kitao K 2000 *Nucl. Data Sheets* **89** 345
[29] Comfort J R 1970 *Argonne National Laboratory Physics Division Informal Report* No. PHY-1970 B (unpublished)
[30] Erb K A and Bhatia T S 1973 *Phys. Rev.* C **7** 2500
[31] Oelrich I C, Krien K, Del Vecchio R M and Neumann R A 1976 *Phys. Rev.* C **14** 563
[32] Igarashi M 1977 Computer code TWOFNR (unpublished)
[33] Perey F G 1963 *Phys. Rev.* **131** 745
[34] Fleming D G, Blann M, Fulbright H W and Robbins J A 1970 *Nucl. Phys.* A **157** 1
[35] Guazzoni P *et al* 1999 *Phys. Rev.* C **60** 054603
[36] Cata-Danil G *et al* 1996 *J. Phys. G: Nucl. Part. Phys.* **22** 107
[37] Guazzoni P, Zetta L, Covello A, Gargano A, Graw G, Hertenberger R, Wirth H-F and Jaskóla M 2004 *Phys. Rev.* C **69** 024619
[38] Guazzoni P, Zetta L, Covello A, Gargano A, Bayman B F, Graw G, Hertenberger R, Wirth H-F and Jaskóla M 2006 *Phys. Rev.* C **74** 054605
[39] Ball J 1972 *Phys. Rev.* C **6** 2139
[40] Guazzoni P, Zetta L, Gu J N, Vitturi A, Eisermann Y, Graw G, Hertenberger R and Jaskóla M 2002 *Nucl. Phys.* A **697** 611
[41] Bertulani C A and Ponomarev V Yu 1999 *Phys. Rep.* **321** 139